Coupling of Electron Orbital Motion with Rotation in the High Rydberg States of BH

A. T. Gilkison, C. R. Viteri, and E. R. Grant

Department of Chemistry, Purdue University, West Lafayette, Indiana 47907, USA

(Received 28 October 2003; published 30 April 2004)

We have applied optical-optical-optical triple resonance spectroscopy to resolve a system of high Rydberg states in BH that serves quantitatively to characterize a fundamental example of electron-orbital–cation core rotational coupling. The third-color ionization-detected absorption spectrum originating from the photoselected $3s\ B\,^1\Sigma^+$ Rydberg state with vibrational and total angular momentum quantum numbers, $v' = 1$ and $N' = 0$ consists entirely of vibrationally autoionizing resonances for which final $N = 1$ that converge in series to the $BH^+ v^+ = 1$ rotational limits, $N^+ = 0$, 1, and 2. For series with $l = 1$ converging to $N^+ = 0$ and 2, Rydberg orbital and rotational angular momenta couple to systematically perturb level energies and distribute lifetime in a well-isolated two-channel rotronic interaction that spans hundreds of wave numbers.

DOI: 10.1103/PhysRevLett.92.173005 PACS numbers: 33.80.Rv, 34.50.Gb, 34.60.+z, 34.80.Kw

The effort to describe energy flow in isolated molecules has added considerably to our understanding of chemical reactivity and has served for years as a major focus of research in chemical physics [1]. Particularly important among pathways for unimolecular decay is the transfer of energy between electronic and internuclear degrees of freedom [2]. Non-Born-Oppenheimer dynamics give rise to significant chemical and physical consequences [3–5], and issues associated with the energy transfer between electronic coordinates and internuclear ones underlie contemporary efforts to control paths of intramolecular relaxation and externally direct the outcomes of chemical transformations [6–9].

Electronic relaxation pathways that exist in molecules excited to levels near and above their first ionization thresholds provide a particularly well-defined set of model non-Born-Oppenheimer processes [10–12]. Here, wave packet dynamics associated with intramolecular energy transfer pathways leading to electron ejection or electron capture can be conveniently framed in terms of coupling between approximately separable orbital-electronic and cation-core internal degrees of freedom [13]. These dynamics are important because they are universal; all molecules ionize. Specific interactions encountered in this regime relate to the elementary dynamics of electron transfer [14] and connect directly with theories of electron-cation inelastic scattering [11,15,16]. Dynamics linking electron motion with heavy-particle vibration and rotation play a decisive role in the process of dissociative recombination [17–19] and regulate the properties of molecular and quasimolecular condensates such as ultracold neutral plasmas [20–22] and Rydberg gases [23–25].

Recent experiments in the time domain have exploited the simple properties of noninteracting Rydberg electron wave functions to devise intuitive interfering pulse sequences to control heavy-particle motion in diatomic rotronic wave packets [26]. There is interest now in extending optical control to systems in which Rydberg series are coupled [27]. Strategies employing rational pulse shapes can succeed in cases for which the rotational-electronic structure is well understood. However, the rovibrational electronic coupling patterns present in most molecules form numerous channels of interaction. High densities of interacting states produce irregular spectra that require a comprehensive multichannel approach for interpretation [28] and call for complex waveforms, guided perhaps by learning algorithms, to achieve control. Photoselection achieved by means of double resonance can isolate transition manifolds by Franck-Condon factors and angular momentum selection rules, but few examples outside of H_2 or N_2 [29–31] have been found in which simple two-state interactions drive straightforwardly recognizable coupling dynamics.

Now in the boron monohydride radical, BH, we have found a molecule of elementary simplicity in which a single well-defined interaction between internuclear and electronic degrees of freedom extends systematically to affect level energies over an interval of more than 1000 cm^{-1}. Confined by triple resonance to transitions originating from the single rovibronic state, $B\,^1\Sigma^+\ v' = 1$, $N' = 0$, this system presents a manifold of entirely $N = 1$ high Rydberg states that lies between the $v^+ = 0$ adiabatic threshold and the $v^+ = 1$ vertical limit. These states form three prominent series in which irregularities that appear atomiclike in a Lu-Fano plot serve to characterize a well-isolated two-channel interaction between rotational and electronic orbital angular momentum.

B_2H_6 seeded at 5% in H_2 is introduced from a stagnation pressure of 3 atm through a solenoid nozzle operated at 10 Hz into a vacuum maintained at 10^{-6} torr. The focused 50 mJ output of a 193 nm excimer laser crosses the pulsed expansion at the nozzle exit. BH radicals produced by photolysis travel 13 cm to reach the ion collection region of a laser photoionization source time-of-flight mass spectrometer.

Two-color state selection isolates single rovibrational levels of the $3s\ B\,^1\Sigma^+$ gateway Rydberg state of BH from which to originate Franck-Condon vertical third-color transitions to manifolds of high Rydberg states. A first photon (ω_1) produced by a Nd:YAG pumped optical parametric oscillator set to 23 097.81 cm^{-1} excites BH from the ground state $X\,^1\Sigma^+$ ($v = 0$, $N = 0$) to the $N = 1$ rotational energy level of the first vibrational level ($v = 0$) of the $A\,^1\Pi$ state. A second unfocused laser pulse (ω_2) from the beta-barium borate doubled output of an excimer pumped dye laser (ω_2) tuned to 31 497.06 cm^{-1} excites BH from this selected rovibronic level of the $A\,^1\Pi$ state in a $P(1)$ transition to the $N' = 0$ rotational energy level of the $B\,^1\Sigma^+$ ($v' = 1$) state. Subsequent excitation from this photoselected level by a third counterpropagating excimer pumped dye laser pulse (ω_3) populates vibrationally autoionizing states converging strictly to Franck-Condon allowed BH^+ $v^+ = 1$ with total angular momentum confined by selection rules to $N = 1$.

The time-of-flight mass spectrometer operates with zero electrostatic field during this photoexcitation sequence. A 400 V pulsed field, applied ~40 ns after the probe lasers, extracts ions into a 1 m Wiley-McClaren flight tube. The ion signal collected by a two-stage microchannel plate detector is conditioned by a $\times 10$ preamplifier and then averaged by a digital oscilloscope. A laboratory computer records this signal as a function of ω_3. The dye laser and optical parametric oscillator wavelengths are calibrated optogalvanically using a Fischer Scientific Fe/Ne hollow cathode lamp.

Figure 1 shows an ionization-detected spectrum of transitions originating from the $N' = 0$ rotational level of the $B\,^1\Sigma^+$ $v' = 1$ state that spans the interval from the $v^+ = 0$ (adiabatic) ionization threshold to the $v^+ = 1$ (vertical) limit. This spectrum displays an overall pattern of converging structure, which for lower energies forms distinctive patterns, consisting of pairs of resonances of varying width that flank sharp central features. These resonances obviously represent Rydberg states built on a $v^+ = 1$ core that decay to the continuum of a vibrational ground state cation plus free electron.

The sharp central features form an evident series fitting with the Hund's case (d) Rydberg formula,

$$E_n = IP_{N^+} - \frac{R}{\nu^2} \tag{1}$$

in which the effective principal quantum number ν, is defined by

$$\nu = n - \delta_{N^+}. \tag{2}$$

This series converges to a third-photon energy of 26 944.7 cm^{-1} with a phenomenological quantum defect, δ_{N^+}, that is approximately constant at 0.907. The angular momentum selection rule for transitions from $N' = 0$ requires that all final states in this spectrum have the total angular momentum value, $N = 1$. The relatively large quantum defect found for this series suggests a penetrating Rydberg orbital. Assigning the series on these grounds to $l = 0$, requires it to converge to the cation rotational state $N^+ = 1$.

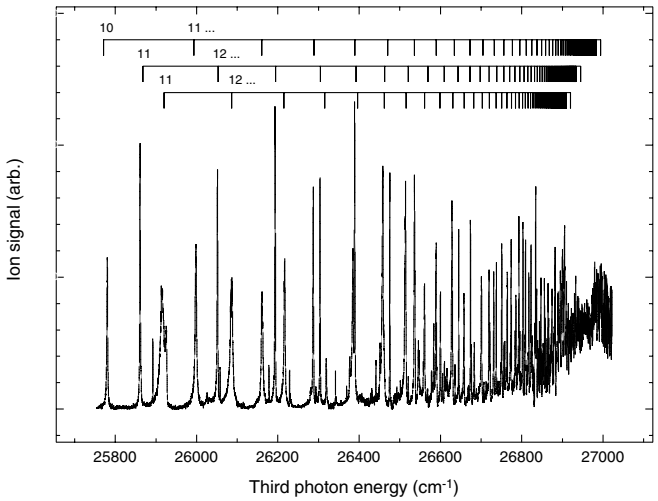

FIG. 1. Ionization-detected absorption spectrum of transitions in BH that originate from the $3s\ B\,^1\Sigma^+$ Rydberg level with vibrational and total angular momentum quantum numbers, $v' = 1$ and $N' = 0$. Ladders labeled by principal quantum numbers mark unperturbed Rydberg series of constant quantum defects, $\delta = 0.526$, 0.907, and 0.529, converging, respectively, to BH^+ $v^+ = 1$ rotational states $N^+ = 0$, 1, and 2 at third photon energies of 26 920.0, 26 944.7, and 26 994.2 cm^{-1}.

The spectrum presents no other features that can be assigned to this limit. However, other limits can be readily derived for testing. The rotational constants of BH^+ are well known from emission spectroscopy [32]. Assuming that the threshold to which the sharp series converges does correspond to $N^+ = 1$, we can estimate the third-photon energy positions of $N^+ = 0$ (26 920.0 cm^{-1}) and $N^+ = 2$ (26 994.2 cm^{-1}). Testing these limits, we find that a series starting with the lower-frequency member of the evident low-energy cluster converges to the BH^+ $v^+ = 1$ limit for which $N^+ = 2$, and one that includes the higher-frequency feature converges to $N^+ = 0$. These series both exhibit average quantum defects of about 0.53, an intermediate value, which is consistent with the orbital angular momentum, $l = 1$, required to achieve final $N = 1$ for these two cation-core rotational states. Perturbations, however, are evident. Quantum defects vary with n, and in the center of the autoionizing interval where the two series coincide, it becomes difficult to assign features to one series or the other.

Under comparable circumstances in atomic systems, similar perturbations, arising from interactions between series built on orbitally coupled configurations of the core, can be compactly described in terms of a graphical representation introduced by Lu and Fano [33]. To construct a Lu-Fano plot, one plots pairs of effective principal quantum numbers or, as in this case, quantum

defects for all the resonances in an interacting pair of series with respect to the ionization thresholds corresponding to both active core configurations.

Figure 2(a) shows a Lu-Fano plot of experimental resonance positions in the spectra of $N = 1$ Rydberg series in BH converging to $^2\Sigma^+$ $v^+ = 1$ cation levels, $N^+ = 0$ and 2 as points in black. For reference, we also show coordinates in gray for similar pairs determined from the resonance positions of series with constant quantum defects $\delta_0 = \tilde{\mu}_o = 0.526$ and $\delta_2 = \tilde{\mu}_2 = 0.529$ that define the corresponding ladders in Fig. 1. A symmetrical avoided crossing in the experimental data reflects the perturbation evident in the spectrum where the series cross in the center of the vibrational autoionization interval. The width of this avoided crossing relates to the strength of the rotational-electronic interaction.

In more formal terms, radial convergence requires the energy levels of a multichannel Coulomb system to satisfy

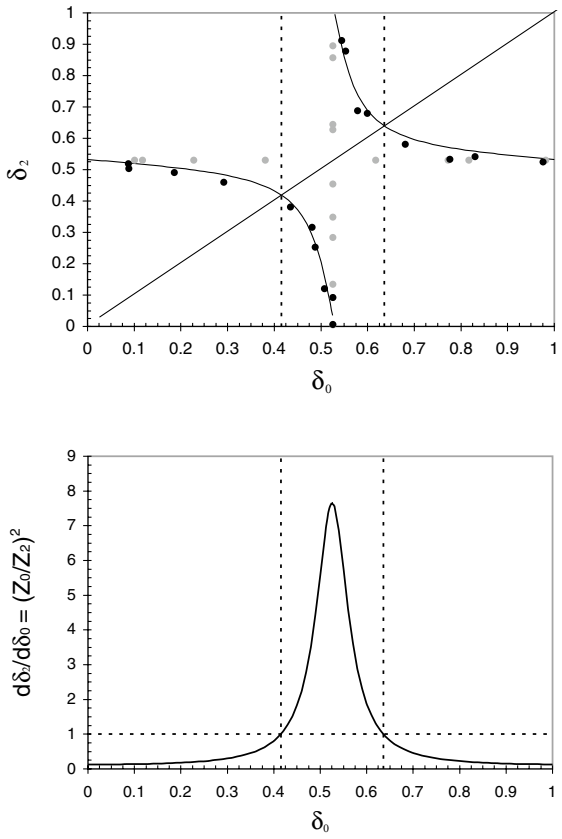

FIG. 2. (a) Top. Lu-Fano plot of quantum defects derived from the experimental positions of resonances assigned to BH series converging to BH^+ $v^+ = 1$ limits, $N^+ = 0$ and 2 (dark points). The light points show a reference plot of defect pairs derived from positions in unperturbed Rydberg series converging to $N^+ = 0$ and 2, pictured as ladders in Fig. 1. The hyperbola is drawn from Eq. (5) for $\xi = 0.36$. (b) Bottom. Plot of the ratio of fragmentation channel amplitudes in the region of the avoided crossing, as determined by Eq. (6) for the coupling parameter, $\xi = 0.36$, derived from the fit in (a).

the determinantal equation [34],

$$\det|\delta_{ij}\tan\pi\nu_i + R_{ij}| = 0, \tag{3}$$

where R_{ij} is a reactance matrix that describes short range Rydberg electron-core interactions, in this case, the coupling of orbital electron and rotational angular momentum. A translation $\nu_i \rightarrow \nu_i + \tilde{\mu}_i$ in ν_i space, which simply renormalizes the radial basis functions in each channel, reduces the reaction matrix into a purely coupling matrix without diagonal elements [35], given by

$$\tilde{R} = \begin{bmatrix} 0 & \xi \\ \xi & 0 \end{bmatrix}, \tag{4}$$

where a dimensionless quantity, $0 \leq \xi \leq 1$, represents the interchannel mixing coefficient.

Expanding Eq. (3) and writing effective principal quantum numbers explicitly in terms of phenomenological quantum defects in the manner of Eq. (2), we obtain the function $\delta_i(\delta_j)$ as it appears in Fig. 2(a):

$$\tan\pi(\tilde{\mu}_0 - \delta_0)\tan\pi(\tilde{\mu}_2 - \delta_2) - \xi^2 = 0. \tag{5}$$

In the absence of interaction, this hyperbolic function would appear as a cross, reflecting quantum defects, δ_i, that are constant and thus independent. A fit of the observed defect pairs for $N^+ = 0$ versus 2 to Eq. (5) yields a value for the coupling constant of $\xi = 0.36$. By contrast, when we combine resonant positions associated with either $N^+ = 0$ or 2 with the energies of features that converge to $N^+ = 1$, we find minima in the χ^2 space of Eq. (5) for $\xi = 0$.

As shown by Giusti-Suzor and Fano [35], the slopes of curves fit to Eq. (5), such as those plotted here for the BH^+ limits, $N^+ = 0$ and 2, describe the ratio of the fragmentation channel amplitudes (Z_0/Z_2) as

$$\frac{d\delta_2}{d\delta_0} = \left(\frac{Z_0}{Z_2}\right)^2 = [\xi^2\cos^2\pi(\tilde{\mu}_0 - \delta_0) + \xi^{-2}\sin^2\pi(\tilde{\mu}_0 - \delta_0)]^{-1}. \tag{6}$$

This ratio, which parallels the admixture of each channel in the eigenstates of the core potential, attains a value of 1 at the points in the continuous space of δ_i where the two branches most nearly meet. The half-width of the function $d\delta_2/d\delta_0$ at this point, denoted by η, describes the displacement of series positions in quantum defect space, $\tilde{\mu}_i \pm \eta$, at the point of closest approach in the two branches of the plot. This parameter relates to the coupling constant according to $\xi = \tan(\pi\eta)$, such that $|\eta| < \frac{1}{4}$. Figure 2(b) illustrates the behavior of the ratio of fragmentation channel amplitudes for the $N^+ = 0$ and 2 series, where we calculate $\eta = 0.11$, reflecting significant interaction.

Clear signs of this interaction can be seen in the spectrum itself. For example, note the shapes of the lines that

form the lowest-frequency cluster of lines in Fig. 1. Flanking the center resonance ($N^+ = 1$, $\nu_i = 10.9$), one finds a sharp feature to lower frequency ($N^+ = 2$, $\nu_i = 9.5$) and a broad one to higher frequency ($N^+ = 0$, $\nu_i = 10.5$). One principal quantum number higher, the flanking resonances exhibit more comparable widths. In the next cluster, the feature to lower frequency appears broader. The quantum defects of these features, and the three sets immediately above, form the avoided crossing in Fig. 2(a).

Thus, for BH we find experimental results pointing directly to channels of electron-orbital–cation core rotational coupling that systematically perturb Rydberg level energies and mix states to alter lifetimes. The fundamental source of line broadening and the channel coupling that distributes it stand now as very well characterized targets for theoretical study and experiments pursuing coherent control.

E. R. G. gratefully acknowledges discussions with Professor A. Suzor-Weiner. This work was supported by the National Science Foundation under Grant No. CHE-0075833.

[1] See, for example, J. Jortner and R. D. Levine, Adv. Chem. Phys. **47**, 1 (1981); R. E. Smalley, Annu. Rev. Phys. Chem. **34**, 129 (1983); T. Uzer, Phys. Rep. **199**, 73 (1991); J. C. Keske and B. H. Pate, Annu. Rev. Phys. Chem. **51**, 323 (2000); M. Gruebele, Adv. Chem. Phys. **114**, 193 (2000).
[2] G. Stock and W. Domcke, Adv. Chem. Phys. **100**, 1 (1997).
[3] I. B. Bersuker, *Electronic Structure and Properties of Transition Metal Compounds* (Wiley, New York, 1996).
[4] E. E. Nikitin, Annu. Rev. Phys. Chem. **50**, 129 (1999).
[5] S. Adhikari and G. Due Billing, Adv. Chem. Phys. **124**, 143 (2002).
[6] R. J. Gordon and S. A. Rice, Annu. Rev. Phys. Chem. **48**, 601 (1997).
[7] M. Shapiro, Adv. Chem. Phys. **114**, 123 (2000).
[8] H. Rabitz, R. de Vivie-Riedle, M. Motzkus, and K. Kompa, Science **288**, 824 (2000).
[9] J. R. R. Verlet, V. G. Stavros, R. S. Minns, and H. H. Fielding, Phys. Rev. Lett. **89**, 263004 (2002).
[10] J. Jortner and S. Leach, J. Chim. Phys. Phys.-Chim. Biol. **77**, 7 (1980).
[11] C. H. Greene and Ch. Jungen, Adv. At. Mol. Phys. **21**, 51 (1985).
[12] S. Mahapatra and H. Köppel, Phys. Rev. Lett. **81**, 3116 (1998).
[13] F. Texier and Ch. Jungen, Phys. Rev. Lett. **81**, 4329 (1998).
[14] M. Bixon and J. Jortner, Adv. Chem. Phys. **106**, 35 (1999).
[15] *Molecular Applications of Quantum Defect Theory*, edited by Ch. Jungen (Institute of Physics, Bristol, 1996).
[16] A. Matzkin, Ch. Jungen, and S. C. Ross, Phys. Rev. A **62**, 062511 (2000).
[17] I. F. Schneider, A. E. Orel, and A. Suzor-Weiner, Phys. Rev. Lett. **85**, 3785 (2000).
[18] V. Kokoouline and C. H. Greene, Phys. Rev. A **68**, 012703 (2003).
[19] P. Forck, C. Broude, M. Grieser, D. Habs, J. Kenntner, J. Liebmann, R. Repnow, D. Schwalm, and A. Wolf, Phys. Rev. Lett. **72**, 2002 (1994).
[20] S. Mazevet, L. A. Collins, and J. D. Kress, Phys. Rev. Lett. **88**, 055001 (2002).
[21] F. Robicheaux and J. D. Hanson, Phys. Rev. Lett. **88**, 055002 (2002).
[22] T. F. Gallagher, P. Pillet, M. P. Robinson, B. Laburthe-Tolra, and M. W. Noel, J. Opt. Soc. Am. B **20**, 1091 (2003).
[23] C. H. Greene, A. S. Dickinson, and H. R. Sadeghpour, Phys. Rev. Lett. **85**, 2458 (2000).
[24] C. Boisseau, I. Simbotin, and R. Côté, Phys. Rev. Lett. **88**, 133004 (2002).
[25] A. L. de Oliveira, M. W. Mancini, V. S. Bagnato, and L. G. Marcassa, Phys. Rev. Lett. **90**, 143002 (2003).
[26] R. S. Minns, J. R. R. Verlet, L. J. Watkins, and H. H. Fielding, J. Chem. Phys. **119**, 5842 (2003).
[27] R. S. Minns, R. Patel, J. R. R. Verlet, and H. H. Fielding, Phys. Rev. Lett. **91**, 243601 (2003).
[28] See, for example, S. C. Ross and C. Jungen, Phys. Rev. A **49**, 4353 (1994); **49**, 4364 (1994); **50**, 4618 (1994).
[29] G. Herzberg, Phys. Rev. Lett. **23**, 1081 (1969).
[30] G. Herzberg and Ch. Jungen, J. Mol. Spectrosc. **41**, 425 (1972).
[31] K. P. Huber and Ch. Jungen, J. Chem. Phys. **92**, 850 (1990).
[32] G. M. Almy and R. B. J. Horsfall, Phys. Rev. **51**, 491 (1937).
[33] K. T. Lu and U. Fano, Phys. Rev. A **2**, 81 (1970).
[34] M. J. Seaton, Proc. Phys. Soc. London **88**, 801 (1966).
[35] A. Giusti-Suzor and U. Fano, J. Phys. B **17**, 215 (1984). **17**, 4267 (1984).